

FISSION OF ANTIMONY BY HIGH-ENERGY PROTONS

A. K. LAVRUKHINA, É. E. RAKOVSKII, SU HUNG-KUEI, and S. KHOĬNATSKII

Institute of Geochemistry and Analytical Chemistry, Academy of Sciences, U.S.S.R.

Submitted to JETP editor July 8, 1960

J. Exptl. Theoret. Phys. (U.S.S.R.) 40, 409-418 (February, 1961)

The fission of antimony nuclei induced by 660-Mev protons was studied. The fission yields as functions of A and Z are single-humped curves. The highest production probabilities are obtained for isotopes lying near the nuclear stability line. The fission is mainly symmetric, and is accompanied by the emission of a large number of charged particles. At $E_p = 660$ Mev the total fission cross section is 0.25 mb. Neutron-deficient isotopes are produced relatively more frequently by fissioning antimony than by heavy nuclei. The relative number of asymmetric fissions diminishes with decreasing incident proton energy.

The principal characteristics of fast-proton fission are shown to vary regularly with decreasing Z of the target nucleus.

1. INTRODUCTION

THE fission of medium-weight nuclei ($Z \lesssim 70$) was discovered in 1950 by Dzhelepov, Golovin, and Kazarinov,¹ using the ionization method of detection, in connection with the irradiation of ${}_{45}\text{Rh}$ by 120-Mev neutrons. Radiochemical techniques were used soon afterward to detect individual fragments from the fission of ${}_{29}\text{Cu}$, ${}_{35}\text{Br}$, ${}_{50}\text{Sn}$, ${}_{56}\text{Ba}$,² ${}_{47}\text{Ag}$,^{2,3} and ${}_{57}\text{La}$ ⁴ by high-energy protons. However, the principal characteristics of fission in medium-weight nuclei have hitherto not been determined. Shamov's recent work,⁵ in which nuclear emulsions were used to investigate Ag fission induced by 330 - 660-Mev protons cannot entirely fill the gap in our knowledge, since the acquired statistics did not provide an adequate basis for unequivocal conclusions.

The present situation results from difficulties in identifying the fission fragments of light nuclei, which are formed with considerably smaller probability than the products of competing nuclear reactions.

The present work investigates the products of the fission of antimony ($Z = 51$) induced by high-energy protons, with the aim of determining the principal characteristics of the fission process (the mass spectrum, isotopic distribution of fragments, nuclear charge distribution, and cross section).

2. EXPERIMENTAL TECHNIQUE

Special care was taken to prepare a pure target. It is known from the literature that cross sections

for the production of individual fragments from fissioning medium-weight nuclei are in the range $10^{-29} - 10^{-30}$ cm². Therefore when the target contains as little as $10^{-3}\%$ of the elements represented by the fission fragments or neighboring elements, the measured activities of individual radioactive fragments are considerably exaggerated. The targets were prepared from an ingot of metallic antimony after several purifications by the zone melting technique used in semiconductor technology. Spectral analysis performed by two different methods failed to detect impurity lines. The antimony was also analyzed by neutron activation. These experiments were performed by one of the present authors in collaboration with Yu. V. Yakovlev and L. A. Smakhtin. The following preliminary results show that the antimony did not contain amounts of impurities sufficient to affect appreciably the yields of its fission fragments:

Impurity element:	Mn	Cu	Zn	As	P	Cr	Ga
Content, %:	$3 \cdot 10^{-6}$	$3.5 \cdot 10^{-6}$	$8 \cdot 10^{-7}$	$4 \cdot 10^{-5}$	$8 \cdot 10^{-6}$	$5 \cdot 10^{-4}$	$3 \cdot 10^{-7}$

Samples of metallic antimony (0.5 - 1 g) were bombarded for one-half to three hours in the internal beam of the synchrocyclotron at the Laboratory of Nuclear Problems of the Joint Institute for Nuclear Research. The aluminum foil wrapping of the samples served to monitor the proton flux by the reaction $\text{Al}^{27}(p, 3p_n)\text{Na}^{24}$, the cross section for which was taken to be 10 mb. Elements with atomic numbers from 11 to 37 were separated chemically. Special attention was devoted to developing in advance the most reliable techniques for separating fission fragments in

Table I. Yields of identified fragments from antimony bombarded with 660-Mev protons

Element	Mass number, A	Decay mode	$T_{1/2}$, experimental	$T_{1/2}$, experimental	$\bar{\sigma}$, 10^{-30} cm ²
¹¹ Na	24	β^-	14,5 hrs.	15 hrs	95 (2)**
¹² Mg	28	β^-	21,5 hrs	21,2 hrs	9,0 (4)
¹⁵ P	32	β^-	14,1 days	14,3 days	3,0*
¹⁶ S	38	β^-	~ 3 hrs	2,9 hrs	0,7 (2)
¹⁷ Cl	38	β^-	~34 min	37,3 min	5,7 (3)
	39	β^-	58 min	55,5 min	1,2 (3)
¹⁹ K	43	β^-	~ 1 days	22,4 hrs	8,0 (3)
²⁰ Ca	47	β^-	~ 6 days	~5 days	3,5 (3)
²² Ti	45	β^+ , EC***	3,2 hrs	3,1 hrs	5,8 (3)
²³ V	48	β^+ , EC	16,7 days	16,0 days	6,8 (7)
²⁴ Cr	48	EC	23,5 hrs	23 hrs	4,0 (5)
²⁵ Mn	56	β^-	2,5 hrs	2,6 hrs	8,3 (3)
²⁶ Fe	59	β^-	~46 days	45,1 days	8,0 (6)
	58 ^m	IT***	9,8 hrs	9 hrs	3,1 (5)
²⁷ Co	61	β^-	~120 min	99-110 min	5,1 (5)
²⁸ Ni	65	β^-	2,7 hrs	2,6 hrs	5,5 (2)
	66	β^-	~60 hrs	55 hrs	2,2 (2)
	62 ^m	EC, β^+	9,3 hrs	9,3 hrs	3,9 (2)
³⁰ Zn	69 ^m	IT	~14,5 hrs	13,8 hrs	15 (2)
	72	β^-	48 hrs	49 hrs	1,1 (2)
³¹ Ga	66	β^+ , EC	9,3 hrs	9,4 hrs	29 (5)
	67	EC	78 hrs	78 hrs	24 (4)
	72	β^-	14,8 hrs	14,3 hrs	3,0 (3)
³⁴ Se	72	EC	9,8 days	~9 days	38 (2)
	73	β^+ , EC	7,1 hrs	7,1 hrs	63 (2)
	75	β^+ , EC	1,6 hrs	1,6 hrs	92 (2)
³⁵ Br	76	β^+	16 hrs	17,2 hrs	32 (2)
	80 ^m	IT	4,3 hrs	4,4 hrs	24 (2)
³⁷ Rb	86	β^-	18-23 days	18,7 days	440 (4)

*Average cross section for P³² production, taking into account certain data communicated privately by L. P. Moskaleva and V. V. Malyshev.

**The number of different determinations of the yield is given in parentheses.

***EC - electron capture; IT - isomer transition.

radiochemically pure form against the background of highly active antimony spallation products, which in many instances resemble the elements to be separated.

The activity of the samples was measured by a type MST-17 end-window counter. Individual radioisotopes were identified from their half-lives, and in some instances from the energy of emitted particles as determined by absorption in the aluminum foil.

A magnetic analyzer was used to determine the sign of the 38-minute activity observed in a chlorine fraction, which could be either β^- emission from Cl³⁸ or β^+ emission from Cl^{34m}. Since positrons were not detected, it was established that the given proton bombardment of Sb produces Cl³⁸ rather than Cl^{34m}.

Extremely weak radioactivities were measured by a setup consisting of type T-25 BFL back-to-back end-window counters in anticoincidence with a ring of MS-9 counters.⁶ This resulted in 5 to 6 times greater efficiency than with end-window counters alone.

The cross sections for radioisotope production were corrected for self-absorption and self-scatter-

ing in the sample, for absorption in air, in the mica windows of counters, and in the wrappings of the samples, for reflection from the backing, and also for a difference in solid angle whenever this last circumstance affected counts from the sample and monitor. In the case of isotopes decaying by electron capture, corrections were also introduced for counting efficiency, absorption in the counter insensitive volume and the fluorescent yield. The accuracy of the cross sections ranged from 50 to 100%.

3. RESULTS AND DISCUSSION

Table I gives the half-lives $T_{1/2}$, the decay modes and average production cross sections $\bar{\sigma}$ of identified products from the bombardment of antimony with 660-Mev protons. Two groups of nuclides were identified (Fig. 1). The region from Rb to Zn ($Z \geq 30$) comprises isotopes formed in antimony spallation. Here the yield diminishes sharply with increase of the difference $\Delta Z = Z_0 - Z$, where Z_0 denotes the atomic number of the original nucleus.

Fission products were found in the region $16 \lesssim Z \lesssim 28$, where the yield was observed to be

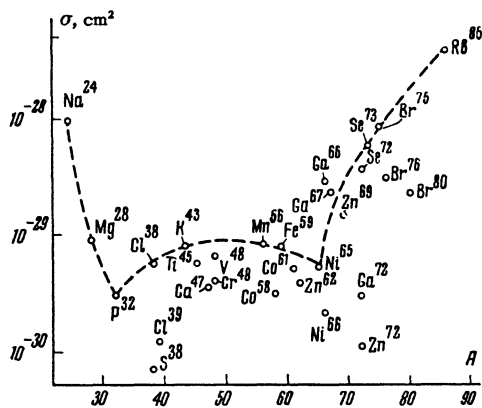


FIG. 1. Yields of identified radioactive products from antimony bombarded with 660-Mev protons.

practically independent of Z . An estimate of the excitation energy E_{exc} required to produce ${}_{23}V^{48}$ by antimony spallation gave ~ 700 Mev for a reaction involving both proton and neutron emission, and ~ 300 Mev for a reaction with α -particle and neutron emission (without considering cascade particles or the variation of the Coulomb barrier as a function of E_{exc}). Practically identical ${}_{23}V^{48}$ yields were obtained with the bombarding energies $E_p = 660$ and 220 Mev. The assignment of the given group to fission is also confirmed by nuclear-emulsion data,⁵ which show a shift ΔZ between the fission-product regions of Ag and Sb representing the difference between the atomic numbers of these two target nuclei.

The yield of Na^{24} , which is considerably larger than that of Sb fission products, can be a result of fragmentation, as indicated by the angular distributions of this isotope when produced by the bombardment of several elements with 660-Mev protons.⁷ Mg^{28} is also evidently formed by this kind of process. The assignment of the identified products of antimony bombardment to groups with different

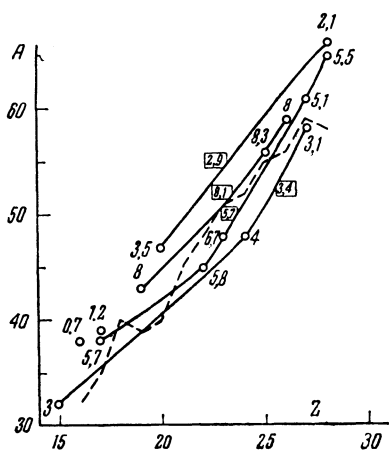


FIG. 2. Yields of radioactive fission products from antimony bombarded with 660-Mev protons. Mean values are enclosed in small boxes.

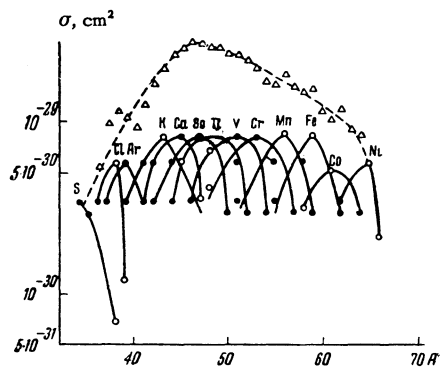


FIG. 3. Fission yields from antimony bombarded with 660-Mev protons as a function of mass number. Dashed curve – total yields; \circ – experimental; \bullet – interpolated; Δ – total yield for each A.

origins is somewhat arbitrary in view of their overlapping.

The yields of the unidentified stable, long- and short-lived radioactive fission fragments of antimony were estimated by interpolation on a plot (Fig. 2) in the coordinates A and Z , where solid lines connect nuclei formed with approximately equal yields. Most of the fission fragments lie very close to the (dashed) nuclear stability line. The cross sections for the formation of a number of unidentified isotopes were obtained by interpolation to within a factor of the order 2. The character of the distribution of antimony fission yields with respect to A and Z was determined from the combined experimental and interpolated data.

The yields are shown in Fig. 3 as a function of mass number. The single-humped curve is similar to those obtained in earlier work^{8,9} for fission fragments of the heavy nuclei U, Th, and Bi. However, differences were observed in the character of the yield distribution. Antimony fission is characterized by the formation of fragments with a broad range of masses for each value of Z , from neutron-rich isotopes to those with relatively large neutron deficiencies, whereas the fission of heavy nuclei results principally in neutron-rich isotopes. The half-width of the humped curves in the latter case is considerably narrower (4–5 mass units) than in the case of antimony (7–8 units).

FIG. 4. Neutron-to-proton ratio of the antimony fission products with the largest yield for each Z .

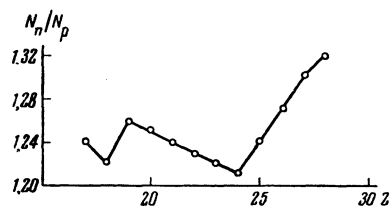


Table II. Characteristics of fission induced by high-energy protons

Target nucleus	E_p , Mev	σ_{fis} , mb	$\sigma_{\text{fis}}/\sigma_{\text{geom}}$	Ratio of neutron deficient, stable, and neutron-rich fragments	Relative number of symmetric fissions, $\sigma_{\text{sym fis}}/\sigma_{\text{fis}}$	No. of emitted protons	No. of emitted neutrons	Reference
1	2	3	4	5	6	7	8	9
^{92}U	480	1650	0.73	11:21:58	0.32	—	19	[9]
^{83}Bi	480	100	$4.8 \cdot 10^{-2}$	12:28:60	0.45	—	15	[9]
^{67}Ho	450	2	$1.1 \cdot 10^{-3}$	—	0.71	4	18	[11]
^{51}Sb	660	0.25	$1.7 \cdot 10^{-4}$	20:35:45	0.73	6—8	16	Present work

The yield peaks from the fission of antimony correspond to the isotopes $^{16}\text{S}^{34}$, $^{17}\text{Cl}^{38}$, $^{18}\text{Ar}^{40}$, $^{19}\text{K}^{43}$, $^{20}\text{Ca}^{45}$, $^{21}\text{Sc}^{47}$, $^{22}\text{Ti}^{49}$, $^{23}\text{V}^{51}$, $^{24}\text{Cr}^{53}$, $^{25}\text{Mn}^{56}$, $^{26}\text{Fe}^{59}$, $^{27}\text{Co}^{62}$, and $^{28}\text{Ni}^{65}$, most of which are stable. Figure 4 shows that the neutron-to-proton ratio N_n/N_p for most of these nuclei lies in the narrow range from 1.22 to 1.27. The only larger ratios are 1.29 for Co^{62} and 1.32 for Ni^{65} .

In the fission of heavy elements the maximum yield is found for isotopes with large neutron deficiencies.

The characteristics of the fission process in antimony result in a marked difference between the isotopic distribution of its fission fragments compared with those of heavy nuclei. Neutron-deficient, stable, and neutron-rich fission fragments of antimony are present in the ratio 20:35:45. The corresponding ratios for Bi, Th, and U,⁷ given in Table II, are 12:28:60, 5:31:64, and 11:21:58, respectively. Antimony fission thus exhibits a considerably larger fraction of neutron-deficient isotopes.

An extensive literature exists on the mass distribution of fission fragments, but very little is known regarding their distribution with respect to nuclear charge. This results from the lack of data on the yields of "screened" isobars* among the fission products. Since the majority of the nuclides identified by us are "screened" isobars under the given experimental conditions, it is surely of interest to study their yields in order to determine the character of the nuclear charge distribution.

Figure 5 shows the charge distribution curves for isobars in the range $A = 37 - 62$. Yields estimated from the curves in Fig. 3 were taken into account. The charge distribution curves, like the mass distribution curves, are single-humped, with

*"Screened" isobars are nuclides which under the given experimental conditions cannot be formed as a result of the decay of other nuclides with the same A.

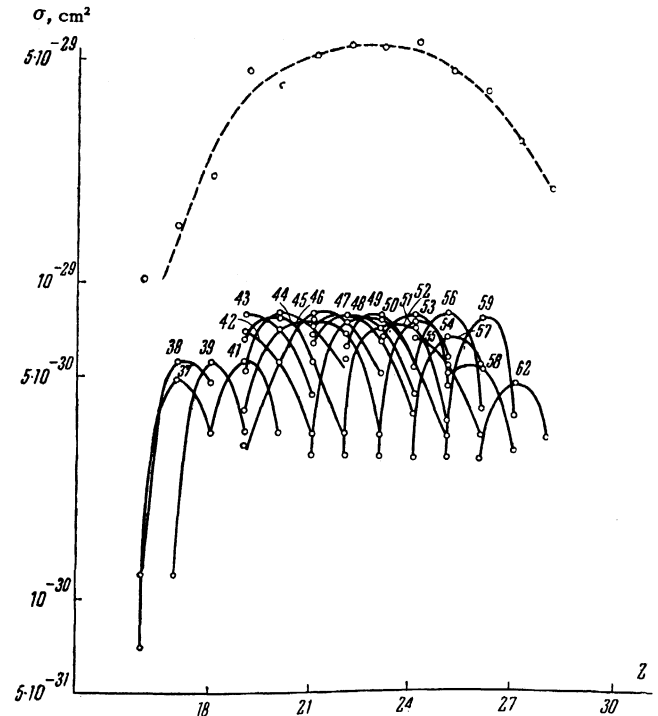


FIG. 5. Yields of isobars from antimony fission induced by 660-Mev protons as a function of atomic number. The dashed curve represents the total yields.

half-widths of three to four charge units. Similar curves plotted for the fission of heavy elements have considerably narrower half-widths (2 or 3 charge units).

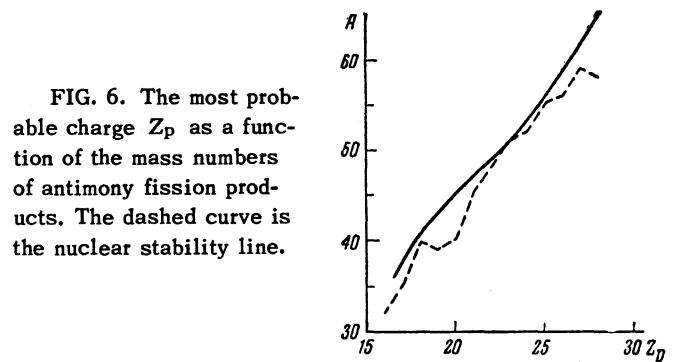


FIG. 6. The most probable charge Z_p as a function of the mass numbers of antimony fission products. The dashed curve is the nuclear stability line.

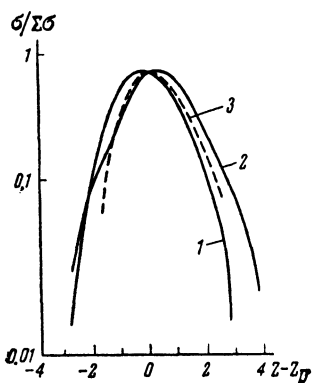


FIG. 7. Fragment charge distribution curves for the fission of (1) U and (2) Bi by 480-Mev protons, and (3) Sb by 660-Mev protons.

The most probable charge Z_p was determined for all isobars in the given range of A , using the same method as in reference 9. The results, given in Fig. 6, show that the curve connecting the most probable charge values is very close to the nuclear stability line. Appreciable departures are observed when the smoothness of the nuclear stability line is disturbed by the exceptionally large relative numbers of nuclides with the magic numbers 20 (Ca^{40}) and 28 (Ni^{58}).

The charge distributions are similar for all isobars. The average curve of charge distribution, plotted in the coordinates $Z - Z_p$ and the fractional yield $\sigma/\Sigma\sigma$ (where $\Sigma\sigma$ is the total yield of isobars with a given value of A , and σ is the yield of each nuclide with the same A), is shown in Fig. 7. A slight preponderance of positive values of $Z - Z_p$ is observed. The fractional yield is ~ 0.4 for the

most probable charge, and ~ 0.05 for the least probable charge. The ratio of the maximum to the minimum fractional yield is one-seventh as large for antimony fission as for heavy-element fission. A similar reduction of the nuclear charge range is observed in heavy-element fission when the bombarding energy is increased.¹⁰ The half-width of the charge distribution curve is 2.5 charge units for antimony fission and 3 units for U and Bi (Fig. 7).

The single-humped curve of the total yields of antimony fragments (the dashed curve in Fig. 5) indicates a large percentage of symmetric fissions, in agreement with Shamov's data.⁵ Symmetric fissions and near-symmetric fissions (when $|Z_{\text{sym}} - Z| \leq 3$) comprise $\sim 73\%$. The three elements Ti, V, and Cr in the middle of the distribution contribute $\sim 34\%$. A similar result is obtained for Ho from an interpolation, like that above, using the data in reference 11. The data in column 6 of Table II show a decreasing proportion of symmetric fissions as Z of the target nucleus increases. Therefore fission asymmetry does not play as large a part in the case of medium-weight nuclei as could be expected from theoretical considerations.¹²

Figure 8 shows the distributions of total yields, with respect to Z , for fragments from Sb fission induced by 660-Mev protons and from the fission of Ho, Bi, and U induced by 450 - 480-Mev pro-

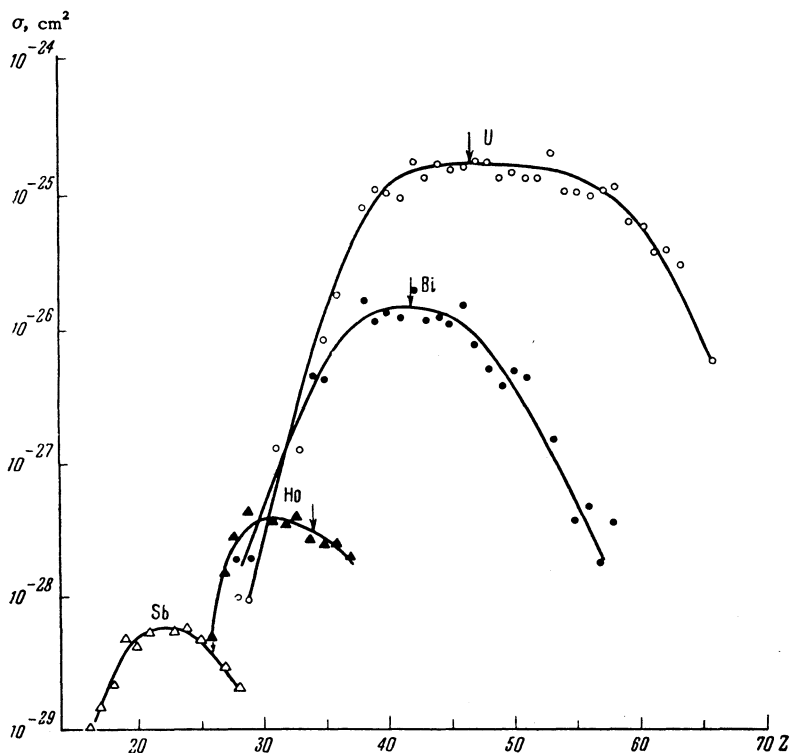


FIG. 8. Total fragment yields from the fission of U, Bi, Ho, and Sb induced by high-energy protons.

tons. The curves are gradually broadened as the target-nucleus charge increases. This is best seen from a comparison of the half-widths, which are 9, 10, 13, and 19 charge units for Sb, Ho, Bi, and U, respectively. The contribution of asymmetric fissions thus increases with Z of the fissioning nucleus. A similar effect from increased bombarding energy had been observed previously.¹³⁻¹⁵ Special experiments showed that for antimony, as for other nuclei, the cross sections for the production of the asymmetric fission products Cl^{38} , Cl^{39} , Mn^{56} , and Co^{61} are reduced to one-tenth or less as the incident proton energy decreases from 660 to 220 Mev, whereas the yield of V^{48} , which is formed in symmetric fission, remains constant in the same proton energy range.

Figure 8 also shows that as Z of the target nucleus decreases the reduced half-widths of the fragment charge distributions are accompanied by a gradual shift of the peaks toward smaller values of Z compared with $Z' = (Z_{\text{init}} + 1)/2$. (In Fig. 8 values of Z' are indicated by arrows.) This indicates that a considerable number of charged particles are emitted in the fission of medium-weight nuclei. The peak of the yield curve for antimony fission (Fig. 5) occurs at Ti ($Z = 22$) and V ($Z = 23$). In symmetric fission the formation of these two nuclei is accompanied by the emission of 6 to 8 protons, including the protons contained in emitted α particles and deuterons. The most probable number of emitted protons, including the incident proton, in antimony fission is therefore 7. This is in agreement with Shamov's result⁵ $\bar{n}_{\alpha,p} = 6.5$ for Ag fission induced by 660-Mev protons.

Four protons are emitted in the fission of Ho (Table II, column 7). The peaks of the curves for U and Bi in Fig. 8 are located at $Z = (Z_{\text{init}} + 1)/2$. However, earlier data¹⁶ show that $\bar{n}_{\alpha,p} = 0.8$ and 1.2, respectively, in the fission of U and Bi by 660-Mev protons.

The number of emitted charged particles is therefore enhanced with decreasing target-nucleus charge. It would appear that this circumstance should increase the probability for the formation of neutron-rich nuclei. However, as we have seen, neutron-deficient and stable isotopes play a relatively large part in antimony fission; this indicates the emission of a large number of neutrons in addition to protons. A calculation shows that the most probable antimony fission mode is accompanied by the emission of 15 to 17 neutrons.

The data in column 8 of Table II show that the number of emitted neutrons is practically independent of the target-nucleus atomic number.

It should be noted that the increased number of fission particles, especially protons, clearly indicates very high excitation energies for fissioning medium-weight nuclei.

A comparison of the curves in Fig. 8 shows that the fission yields from antimony are considerably smaller than from heavy nuclei. The total cross section for antimony fission by 660-Mev protons is 0.25 mb, which is 1.7×10^{-4} of the geometric cross section calculated from $R = r_0 A^{1/3}$, with $r_0 = 1.37 \times 10^{-13}$ cm.¹⁷ The probability of fission increases greatly with Z of the target nucleus. Thus the cross section for uranium fission is 6600 times larger than that for antimony fission. Columns 3 and 4 of Table II show that fission is a dominant nuclear process in heavy elements. Our value for the antimony fission cross section is comparable with that obtained for the fission of silver (0.32 mb)⁴ induced by protons with the same energy.

The foregoing data indicate that the variation of Z of the target nucleus is accompanied by regular variations of all fundamental fission parameters — cross sections, fragment distributions with respect to A and Z , isotopic distribution of the fragments etc., undoubtedly as a result of variation in the character of the fission process. It is currently believed that emissive fission predominates in the heaviest nuclei,¹⁸ that fission from an excited level increases as Z is reduced, and that for antimony and neighboring elements the latter type of fission is obviously dominant.

The authors are deeply indebted to V. N. Mekhedov and T. V. Malysheva for valuable advice, and to L. D. Revina, L. D. Firsova, and I. S. Kalicheva for experimental assistance.

¹ V. P. Dzhelepov and B. Pontecorvo, *Атомная энергия (Atomic Energy)* **3**, 413 (1957).

² R. E. Butzel and G. T. Seaborg, *Phys. Rev.* **82**, 607 (1951).

³ Kurchatov, Mekhedov, Borisova, Kuznetsova, Kurchatova, and Chistyakov, Conference of the U.S.S.R. Academy of Sciences on the Peaceful Uses of Atomic Energy, Session of the Division of Chemical Sciences, Acad. Sci. Press, 1955, p. 178.

⁴ Lavrukhina, Krasavina, and Pozdnyakov, *Doklady Akad. Nauk S.S.S.R.* **119**, 56 (1958), *Soviet Phys.-Doklady* **3**, 283 (1958).

⁵ V. Shamov, *JETP* **35**, 316 (1958), *Soviet Phys. JETP* **8**, 219 (1959).

⁶ V. Varanov and L. Moskaleva, *Заводская лаборатория (Factory Laboratory)* in press.

⁷ Lavrukhina, Moskaleva, Malyshev, Satarova, and Su Hung-Kuei, JETP **38**, 994 (1960), Soviet Phys. JETP **11**, 715 (1960).

⁸ A. Lavrukhina, Doctoral Dissertaion, Institute of Geochemistry and Analytical Chemistry, U.S.S.R. Acad. Sci., 1955.

⁹ A. Lavrukhina and L. Krasavina, Атомная энергия (Atomic Energy) **2**, 27 (1957).

¹⁰ Pate, Foster, and Yaffe, Can. J. Chem. **36**, 1691 (1958).

¹¹ P. Kruger and N. Sugarman, Phys. Rev. **99**, 1459 (1955).

¹² B. Geilikman, Collection, Физика деления атомных ядер (The Physics of Atomic Fission), Moscow, 1957, p. 4.

¹³ Perfilov, Ivanova, Lozhkin, Ostroumov, and Shamov, op. cit. ref. 3, p. 79.

¹⁴ Murin, Preobrazhenskii, Yutlandov, and Yaki-mov, *ibid.*, p. 160.

¹⁵ Lavrukhina, Revina, and Rakovskii, Doklady Akad. Nauk S.S.S.R. **125**, 532 (1959), Soviet Phys.-Doklady **4**, 361 (1959).

¹⁶ A. Lavrukhina, Успехи химии (Progress in Chemistry) **22**, 517 (1958).

¹⁷ V. I. Moskalev and B. V. Gavrilovskii, Doklady Akad. Nauk S.S.S.R. **110**, 972 (1956), Soviet Phys.-Doklady **1**, 607 (1956).

¹⁸ Perfilov, Lozhkin, and Shamov, Usp. Fiz. Nauk **70**, 3 (1960), Soviet Phys.-Uspekhi **3**, 1 (1960).

Translated by I. Emin